AFRL-DE-TR-2000-1044

AFRL-DE-TR-
2000-1044

Electrical Breakdown of Hydrogen and Helium on Subnanosecond Time Scales

J. M. Gahl et al.

The University of New Mexico
Department of Electrical and Computer Engineering
Albuquerque, New Mexico 87131

August 2000

Final Report

AIR FORCE RESEARCH LABORATORY
Directed Energy Directorate
3550 Aberdeen Ave SE
AIR FORCE MATERIEL COMMAND
KIRTLAND AIR FORCE BASE, NM 87117-5776

AFRL-DE-TR-2000-1044

If you change your address, wish to be removed from this mailing list, or your organization no longer employs the addressee, please notify AFRL/DEHP, 3550 Aberdeen Ave SE, Kirtland AFB, NM 87117-5776.

This report has been approved for publication.

William D Prather
WILLIAM D. PRATHER, DR-IV
Project Manager

FOR THE COMMANDER

Mark R Fra
MARK FRANZ, Lt Col, USAF
Chief, High Power Microwave Division

R Earl Good
R. EARL GOOD, SES
Director, Directed Energy

REPORT DOCUMENTATION PAGE

Form Approved
OMB No. 074-0188

1. AGENCY USE ONLY (Leave blank)

2. REPORT DATE
Aug 00

3. REPORT TYPE AND DATES COVERED
Final Report, 24 Dec 97 – 15 Jun 99

4. TITLE AND SUBTITLE
Electrical Breakdown of Hydrogen and Helium on Subnanosecond Time Scales

5. FUNDING NUMBERS
C: F29601-98-2-0003
PE: 61102F
PR: 2304
TA: AK
WU:AB

6. AUTHOR(S)
**D. W. Scholfield, ***N. Shimomura, *J. M. Gahl and J. Lester

7. PERFORMING ORGANIZATION NAME(S) AND ADDRESS(ES)

*The University of New Mexico
Department of Electrical and Computer Engineering
Albuquerque, New Mexico 87131

8. PERFORMING ORGANIZATION REPORT NUMBER

9. SPONSORING / MONITORING AGENCY NAME(S) AND ADDRESS(ES)

**Air Force Research Laboratory / Directed Energy
3550 Aberdeen Ave, SE
Kirtland AFB, NM 87117-5776
William D Prather (505)846-0416

10. SPONSORING / MONITORING AGENCY REPORT NUMBER
AFRL-DE-TR-2000-1044

11. SUPPLEMENTARY NOTES
* * * Department of Electrical and Electronics Engineering, The University of Tokushima, Japan

12a. DISTRIBUTION / AVAILABILITY STATEMENT
Approved for Public Release; Distribution is Unlimited.

12b. DISTRIBUTION CODE

13. ABSTRACT ***(Maximum 200 Words)***

This report describes the experimental determination of the formative time lag data for hydrogen and helium. For subnanosecond risetime pulses, there are typically very few free electrons in the discharge space generated through ionization by external radiation sources such as cosmic rays. Therefore, electrical field emission plays a very important role in these discharges. This report also includes a theoretical determination of the effective electric field for an arbitrary electromagnetic pulse. The effective electric fields for a variety of pulse shapes are calculated for the first time.

14. SUBJECT TERMS
Subnanosecond, Breakdown, Pulse

15. NUMBER OF PAGES
26

16. PRICE CODE

17. SECURITY CLASSIFICATION OF REPORT
UNCLASSIFIED

18. SECURITY CLASSIFICATION OF THIS PAGE
UNCLASSIFIED

19. SECURITY CLASSIFICATION OF ABSTRACT
UNCLASSIFIED

20. LIMITATION OF ABSTRACT
UNLIMITED

NSN 7540-01-280-5500

Standard Form 298 (Rev. 2-89)
Prescribed by ANSI Std. Z39-18
298-102

Table Of Contents

Table Of Figures

Electrical Breakdown of Hydrogen and Helium on Subnanosecond Time Scales

N. Shimomura

Department of Electrical and Electronics Engineering

The University of Tokushima, JAPAN

D. W. Scholfield

Directed Energy Directorate

Air Force Research Laboratory

J. M. Gahl and J. Lester

Department of Electrical and Computer Engineering

The University of New Mexico

One of the major drivers of pulsed power innovation is ultra-wide-band technology. Subnanosecond risetimes with nanosecond or less pulse duration place this technology in a temporal regime that corresponds to microwave frequencies. The ultra-wide-band devices used in this region have pushed pulsed power technology into a parameter space where there is little published data on breakdown. This paper describes the experimental determination of the formative time lag data for two gases, hydrogen and helium, under the application of intense, transient, electric fields. The experiment depicted utilized the Hindenberg series of hydrogen-gas switched pulsers at the Air Force Research Laboratory located at Kirtland Air Force Base. For subnanosecond risetime pulses, there are typically very few free electrons in the discharge space generated through ionization by external radiation sources such as cosmic rays. Therefore, electric field emission plays a very important role in these discharges. However, a small number of discharges are affected by ionization from external radiation, with the resulting data lying between the classic formative time lag curves and the limit set by field emission. As a verification of this effect, an intense, continuous, UV source was utilized for supplying seed electrons and the expected formative time lag curves of Hydrogen and Helium were obtained.

Introduction

Interest in gas breakdown phenomena for fast risetime pulses has recently increased. Subnanosecond risetimes with nanosecond or less pulse duration place the results of this technology in a temporal regime that corresponds to microwave frequencies. The breakdown phenomena in High Power Microwave (HPM) machines and their supporting equipment, such as vacuum windows, is a critical matter for HPM development. Additionally, in order to obtain fast switching in pulsed power devices, basic breakdown phenomena must be studied. Paschen and breakdown time lag curves have been used to characterize breakdown phenomena in various gases in pulsed as well as DC conditions. Several theoretical studies have derived the breakdown curves for pulsed fields [1], especially in molecular nitrogen. In other studies relativistic effects have been taken into consideration [2]. Breakdown curves have also been obtained in experimental studies by using continuous microwave sources [3]-[6] and pulsers [7],[8]. However, these experiments did not provide as much temporal information as the theoretical studies because of the absence of pulsers with extremely fast risetimes.

In this paper, electromagnetic transient phenomena of gas in a subnanosecond time regime, as well as the formative time lag curves of hydrogen and helium gas under these conditions, are presented. This work utilized the Hindenberg series of hydrogen-gas switched pulsers at the Air Force Research Laboratory (AFRL), located at Kirtland Air Force Base.

Experimental Configuration and Diagnostics

Figure 1 shows the experimental configuration. The H2 pulser, one of the Hindenberg series at AFRL, is utilized as the source. Pulses are generated by a transformer with 1:28 windings ratio with an extremely short pulse forming line (PFL) above a peaking-gap switch. The capacitor bank consisting of 8 capacitors (2 nF each, totaling 16 nF), is charged with a high voltage power supply. A gap switch conducts by self-breakdown and the capacitor bank drives the primary coil. The maximum charging voltage of the bank is 30 kV, while the pressure of compressed air in the gap is adjusted to between 0.17 and 0.31 MPa. The pulse forming line is charged by the transformer. The peaking-gap switch consists of two cylindrical electrodes plated with tungst-argent in a high-pressure container. The air in this container is compressed to a pressure of between 3.55 and 7.00 MPa. When the peaking-gap switch breaks, the pulse propagates through a transmission line to an arc chamber. For example, for a charging voltage of 30 kV, pulses having a magnitude of 400 kV and a risetime of approximately 1 ns propagate down the transmission line.

The pulser and the arc chamber are connected by an oil-filled, coaxial transmission line that is 176.5-cm long. In the arc chamber, the inner and outer conductor are 10.2 cm and 17.1 cm in diameter, respectively, and the resulting impedance matches the 40 Ω of the transmission line. Two hemisphere electrodes with diameters of 10.2 cm each are made from aluminum and are separated by an adjustable distance of from 0 to 2.54 cm. Twice the pulse voltage develops on the gap due to the high (open) impedance before an arc discharge. Discharge phenomena occur in the gap at the center of the electrodes. The pressures of the gases, i.e., hydrogen and helium, were varied between 100 mTorr and 1000 Torr in these experiments.

Voltage waveforms are observed with an electric field sensor on the transmission line, whose sensitivity is 3.25 mV / (kV/m). The observed signals are transferred to a screen room through a RG-214 foam flex coaxial cable and a delay line, and are recorded with a scan-converting, digitizing oscilloscope (Tektronix SCD5000, 4.5 GHz bandwidth). The voltage signal is formed by the voltage pulse propagating from the generator with the voltage wave reflected at the arc chamber superimposed. The sensor was placed 87.6 cm away from the arc chamber to accommodate pulse width and transit time. Typical signals obtained with the sensor are shown in Figure 2. Each of the four waveforms is obtained by different helium pressures in the arc chamber. The voltage waves propagating from the generator are observed starting at 2 ns and ending at 8 ns, while the reflected waves at the arc chamber are observed starting at 11 ns.

In Figure 2, various voltage waveforms have been plotted. All waveforms overlay up to 12 ns. They then separate from each other on the basis of pressure. The waveforms in Figure 2 after 12 ns show the reflected pulses from the gap passing the E-probe sensor. The presence of discharge between the electrodes generates different waveforms, therefore, the bifurcation of the traces indicates the beginning of discharge. The time to discharge is directly measured from waveforms. Furthermore, because of capacitance, the voltage between the electrodes is not exactly twice the incident voltage expected at a perfect open circuit.

The waveforms observed with the E-field sensor were recorded on a digitizing oscilloscope. They are converted into voltage waveforms by taking the sensitivity of the sensor and the geometrical configuration of the transmission line into consideration. Furthermore, the voltage at the sensor on the transmission line is obtained by filtering using FFT (and inverse FFT), and a low-pass filter. The transfer function of the cable and the delay line between the sensor and the digitizing oscilloscope were measured with a network analyzer.

Figure 3 shows the equivalent circuit for determining, by numerical analysis, the voltage between the electrodes. The transmission line, the arc chamber, and the electrodes are treated as LC ladder circuits. The gap between the electrodes is assumed to be a capacitor. The inductance and capacitance of the part of the circuit representing the electrode region were evaluated with regard to their configuration, i.e., the electrodes are hemispheres. The voltage waveforms obtained experimentally and filtered were provided as the voltage source at the left end of Figure 3. The circuit simulation was divided into about 2,000 combinations of L and C. The voltage across the gap and the ratio of voltage across the gap to the incident pulse voltage are shown in Figure 4 for a gap length of 1.65 mm. While the incident voltage pulses have 10%-90% risetimes of 0.55 ns, the risetime of the voltage pulse across the gap is 0.98 ns. The voltage across the gap peaks at approximately 1.6 ns and the ratio of voltages is a maximum at 2 ns. The voltage across the gap increases linearly between 0.3 ns and 1.4 ns. The ratios of different gap lengths are calculated in the same way. Each voltage waveform obtained experimentally is multiplied by the ratio and the hold-off voltages are evaluated from the beginning time of the discharge.

Experimental Results and Discussion

An analysis of the generated formative time lag curve is used to investigate the breakdown phenomena in the subnanosecond regime. While the breakdown curves for such fast pulses have had several theoretical analyses, they have not been sufficiently studied experimentally. Cathode design limited the investigation to single-channel discharges.

In order to obtain more accurate formative time curves, the experiment utilized a UV source. The electrodes and their gap space were irradiated by UV light produced by a xenon lamp so that electrons would be present on the electrode prior to pulsing. A 150-W bulb was located at a distance of 40 cm from the center of the electrodes, outside of the arc chamber, and the light was guided to the discharge regime through a lens and a quartz window.

The relationships between E_o/P and Pt for Hydrogen and Helium are shown in Figures 5 and 6, respectively. The solid and open symbols indicate the conditions with and without the UV source. The gap separation between the electrodes was 2.0 mm and the charging voltage of the capacitor bank was 30kV. The formative time curve applies to all gap separations. The various geometric figures within each grouping indicate data taken at a specific gas pressure. Note that data obtained at specific pressures are distributed in a linear manner.

With UV illumination both the curves of Hydrogen and Helium have a shape which is approximately a formative time curve, while the relative positions of the curves are shifted. Without the application of UV light, electric field emission supplies virtually all initial electrons and the data form nearly a straight line. Nevertheless, several breakdown events induced by electrons created by external radiation can be observed, and tracing the outlier data points draws the formative time lag curves. The electric field emission line of Hydrogen corresponds approximately to that of Helium. The data around Pt = 10^-6 Torr·s for Hydrogen are located about the electric field emission line. Under these conditions the formative time lag is considerable, and can not be neglected when the seed electrons are produced by electric field emission. For switching in this time regime electric field emission is the dominant phenomenon for the production of seed electrons, while photo-ionization by external radiation is the secondary mechanism. The data in the lower left corner of the formative time lag curve (for DC systems near the so-called Paschen minimum), denotes a short hold-off time, i.e., the formative time lag is small. Most of the discharges observed in this regime occurred with a longer period than expected due to the absence of seed electrons. The formative phase may become shorter because of the changing applied field. For use in fast switching, good performance can be expected in this region. Since the seed electrons due to photo-ionization are negligible, ultra-fast switching may be possible. In this regime, the choice of electrode material, as well as selection of electrode dimensions would regulate the hold-off voltage.

Conclusion

Breakdown phenomena in the subnanosecond region were observed, with experimentally obtained formative time lag curves presented. The probability of electrons existing during the application of electric fields is extremely low. Electric field emission, consequently,- supplies virtually all initial electrons and the experimental results almost form a straight line. Nevertheless, several breakdown events induced by electrons produced by external radiation such as a cosmic ray can be observed, and tracing the outlier data points draws the formative time lag curves. While the electric-field-emission-induced breakdown is almost independent on the kind of gas (Hydrogen or Helium), the formative time lag curve is affected by the gaseous species. All data are located in a region between the formative time lag curve and the electric field emission curve. An intense continuous UV source was utilized for supplying seed electrons and the expected formative lag curves of Hydrogen and Helium were obtained. For switching application in this time region, electric field emission is the dominant phenomenon of initial electron production when compared to photo-ionization by external radiation.

Acknowledgement

This work was supported by the Air Force Research Laboratory.

References

[1] Y. A. Lupan, Refined Theory for an RF Discharge in Air, Soviet Physics Technical Physics, Vol. 21, No. 11, Nov. 1976.

[2] G. Graham and R. A. Roussel-Dupre', Air Breakdown in the Relativistic Limit, Technical Documentary Report No. CONF-89051841, Los Alamos National Laboratory, Dec. 1989.

[3] A. D. MacDonald, Microwave Breakdown in Gases, Wiley, New York, 1966.

[4] S. J. Tetenbaun, A. D. MacDonald, and H. W. Bandel, Pulse Microwave Breakdown of Air from 1 Torr to 1000 Torr, Journal of Applied Physics, Vol. 42, p. 5871, 1971.

[5] A. W. Ali and T. Coffey, Naval Research Laboratory Memorandum No. 4320, 1980 (unpublished).

[6] C. A. Sullivan, W. W. Destler, J. Rodgers and Z. Segalov, Short-Pulse High-Power Microwave Propagation in the Atmosphere, Journal of Applied Physics, Vol. 63, No. 11, June 1988.

[7] P. Felsenthal and J. M. Pround, Nanosecond Pulse Breakdown in Gases, Physical Review, pp.1796-1804, Sept. 1965.

[8] D. W. Scholfield, J. M. Gahl, and B. W. Mullins, Investigation of the Paschen Curve of Nitrogen via the application of nanosecond pulsed electromagnetic ratiation, Journal of Applied Physics, Vol. 76, No. 3, p.1473, August 1994.

[9] D. W. Scholfield, J. M. Gahl, and Naoyuki Shimomura, Effective Electric Field for an Arbitrary Electromagnetic Pulse, IEEE Transactions on Plasma Science, Vol. 27, No. 2, April 1999

Figure Captions

Fig. 1. Experimental schematic

Fig. 2. Waveforms of E probe signal

Fig. 3. Analysis Circuit

Fig. 4. Voltage across the gap and ratio of voltage across the gaps on incident voltage pulse.

Fig. 5. The relation between E_o/P and Pt for Hydrogen

(Gap separation is 2.0 mm. - Black: with UV, White: w/o UV)

Fig. 6. The relation between E_o/P and Pt for Helium

(Gap separation is 2.0 mm. – Black: with UV, White: w/o UV)

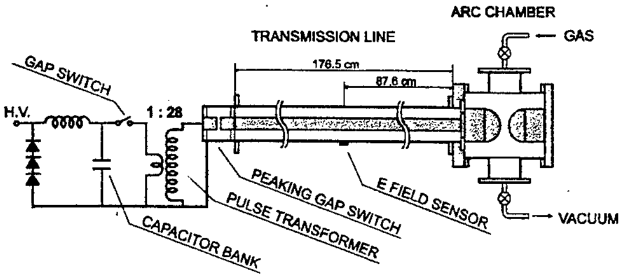

Figure 1. Experimental schematic.

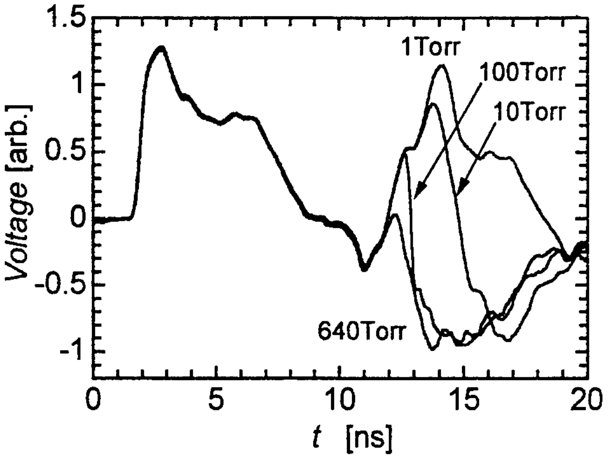

Figure 2. Waveforms of E probe signal.

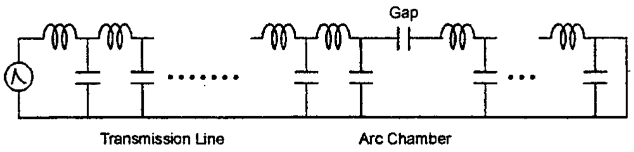

Figure 3. Analysis Circuit.

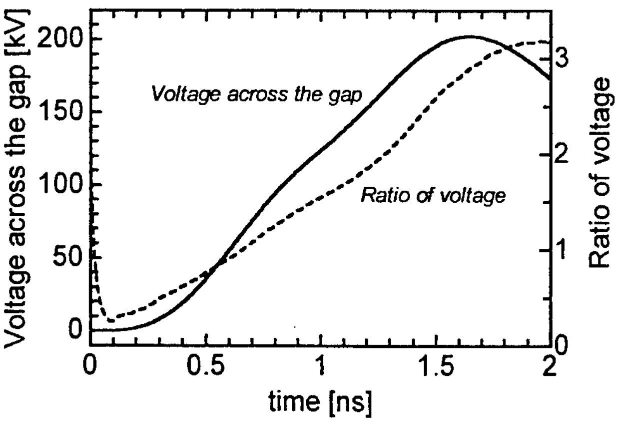

Figure 4. Voltage across the gap and ratio of voltage across the gaps on incident voltage pulse.

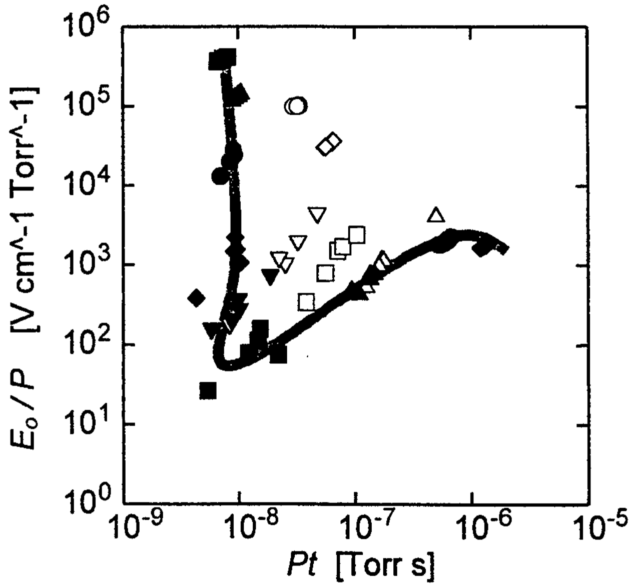

Figure 5. The relation between E_0/P and Pt for Hydrogen.
(The gap separation is 2.0 mm. - Black: with UV, White: w/o UV)

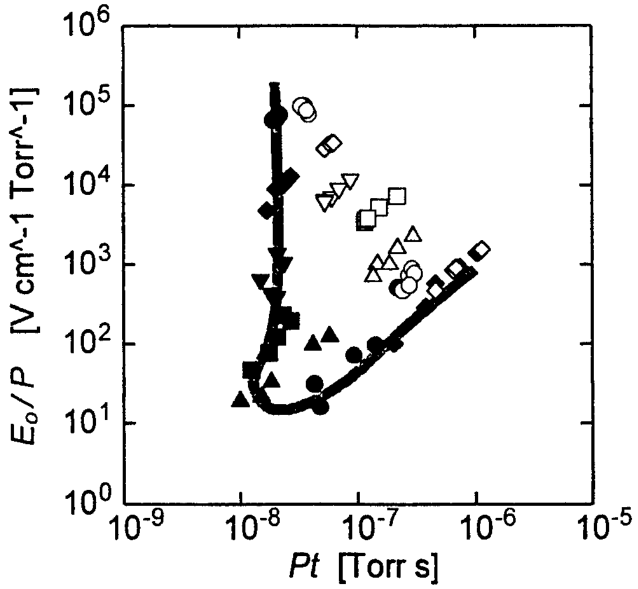

Figure 6. The relation between E_0/P and Pt for Helium.
(The gap separation is 2.0 mm. - Black: with UV, White: w/o UV)

DISTRIBUTION LIST

DTIC/OCP 8725 John J. Kingman Rd, Suite 0944 Ft Belvoir, VA 22060-6218	1 cy
AFSAA/SAMI 1570 Air Force Pentagon Washington, DC 20330-1570	1 cy
AFRL/VSIL Kirtland AFB, NM 87117-5776	2 cys
AFRL/VSIH Kirtland AFB, NM 87117-5776	1 cy
AFRL/DE/Chief Scientist Kirtland AFB, NM 87117-5776	1 cy
Official Record Copy AFRL/DEHP/D. W. Scholfield	5 cys